

A novel one-pot ‘green’ synthesis of stable silver nanoparticles using soluble starch

N. Vigneshwaran,* R. P. Nachane, R. H. Balasubramanya and P. V. Varadarajan

Nanotechnology Research Group, Central Institute for Research on Cotton Technology, Adenwala Road, Matunga, Mumbai 400 019, India

Received 24 December 2005; received in revised form 21 April 2006; accepted 25 April 2006

Available online 22 May 2006

Abstract—Stable silver nanoparticles have been synthesized by using soluble starch as both the reducing and stabilizing agents; this reaction was carried out in an autoclave at 15 psi, 121 °C for 5 min. Nanoparticles thus prepared are found to be stable in aqueous solution over a period of three months at room temperature (~25 °C). The size of these nanoparticles was found to be in the range of 10–34 nm as analyzed using transmission electron micrographs. The X-ray diffraction analysis revealed the face-centred cubic (fcc) geometry of silver nanoparticles. Iodometric titration confirmed the entrapment of silver nanoparticles inside the helical amylose chain. These silver nanoparticles embedded in soluble starch produced a typical emission peak at 553 nm when excited at 380 nm. The use of environmentally benign and renewable materials like soluble starch offers numerous benefits of eco-friendliness and compatibility for pharmaceutical and biomedical applications.

© 2006 Elsevier Ltd. All rights reserved.

Keywords: Amylose–iodine complex; Green chemistry; Photoluminescence; Silver nanoparticles; Soluble starch

1. Introduction

Over the past decade, increasing awareness about the environment has led researchers to focus on ‘green chemistry’. Utilization of nontoxic chemicals, environmentally benign solvents and renewable materials are some of the key issues that merit important consideration in a green synthesis strategy.^{1–3} Nanomaterials have wide-ranging implications in a variety of areas, including physics, chemistry, electronics, optics, materials science and the biomedical sciences. In spite of the novel properties exhibited by the metal nanoparticles due to quantum size effects, their synthesis protocol poses a major environmental problem.^{4–6} Most of the synthetic methods reported to date rely heavily on the use of organic solvents and toxic reducing agents like sodium borohydride and *N,N*-dimethylformamide. All these chemicals are highly reactive and pose potential environ-

mental and biological risks. With the increasing interest in minimization/elimination of waste and adoption of sustainable processes through green chemistry, the development of biological, biomimetic and biochemical approaches is desirable. In earlier reports where natural polymers like starch³ and chitosan⁷ are reported to stabilize silver nanoparticles, separate reducing agents were used.

Recently, researchers have begun using biological molecules as templates for generation of inorganic structures and materials. Biological systems form sophisticated mesoscopic and macroscopic structures with tremendous control over the placement of nanoscopic building blocks within extended architectures.⁸ Since the more immediate applications of nanoparticles will be in medical diagnosis and therapeutics like detection of genetic disorders by using gold nanoparticles,^{9,10} colour-coded fluorescent labelling of cells using semiconductor quantum dots¹¹ and cell transfection for gene therapy and drug delivery,¹² the use of biologically compatible materials for nanoparticles synthesis and stabilization will undoubtedly play a crucial role.

* Corresponding author. Tel.: +91 22 24127273; fax: +91 22 24130835; e-mail: nvw75@yahoo.com
URL: www.circot.res.in

The concept of green nanoparticles preparation using β -D-glucose as the reducing agent was first reported by Raveendran et al.³ where starch played the role of stabilizer. In the present work, silver nanoparticles are prepared using soluble starch acting as both the reducing and stabilizing agents. Soluble starch, the amylose component of starch, is a linear polymer formed by the α -(1 \rightarrow 4) linkages between D-glucose units and adopts a left-handed helical conformation in aqueous solution. Despite its slight branching, amylose behaves essentially like a linear polymer, forming films and complexes with ligands.¹³ In this report, the aldehyde terminal of soluble starch is used to reduce silver nitrate while the starch itself stabilized the silver nanoparticles.

2. Materials and methods

2.1. Materials

Soluble starch ($\overline{M}_w = 2200$; $\overline{M}_n = 950$; polydispersity index = 2.3) and silver nitrate were obtained from HiMedia[®] Ltd (India). All chemicals were of analytical grade and used without further purification. All aqueous solutions were made using ultrahigh purity water (18 M Ω cm resistance) purified using a Milli-Q[®] Plus system (Millipore Co.).

2.2. Preparation of silver nanoparticles

In a typical one-step synthesis protocol, 1.0 g of soluble starch was added to 100 mL of deionized water and heated in microwave oven. After complete dissolution, 1 mL of a 100 mM aq solution of silver nitrate was added and stirred well. This mixture was kept in an autoclave at 15 psi pressure, 121 °C for 5 min. The resulting solution was clear yellow in colour indicating the formation of silver nanoparticles.

2.3. UV–visible spectral analysis

The UV–vis spectrum of the silver nanoparticles embedded in soluble starch was recorded in Specord 50 ANALYTIKJENA[®] spectrophotometer, from 200 to 900 nm. A solution containing 1.0% soluble starch was used as the blank.

2.4. Transmission electron microscopy and electron diffraction

For transmission electron microscopy (TEM), a drop of aqueous solution containing the silver nanoparticles embedded in soluble starch was placed on carbon-coated copper grids and dried under infrared lamp. Micrographs were obtained using a Philips[®] EM208

TEM operating at 200 kV. The electron diffraction pattern was also recorded for the selected area.

2.5. Iodimetric titration

The stabilization of silver nanoparticles by soluble starch was analyzed by iodimetric titration. The silver nanoparticles prepared in soluble starch solution (100 mL) was titrated with 0.1 N iodine solution (I₂/KI). At regular intervals, the change in colour was monitored by recording the UV–vis spectrum as mentioned above. Once the stable blue colour was obtained due to the amylose–iodine complex, 50 mL of the nanoparticles solution stabilized with soluble starch was added, and the spectrum was recorded again.

2.6. X-ray diffraction analysis

The aqueous solution of soluble starch embedded with silver nanoparticles was spray dried in a JISL LSD48 Mini Spray Drier at 100 °C, and the brown-coloured powder obtained was used for X-ray diffraction (XRD) analysis. The powder X-ray diffraction was performed using a Phillips[®] PW 1710 X-ray Diffractometer with nickel filtered Cu K α ($\lambda = 1.54$ Å) radiation and analyzed using APD (automatic powder diffraction) software. The diffracted intensities were recorded from 10° to 65° 2 θ angles.

2.7. Photoluminescence analysis

Photoluminescence spectra were recorded in Perkin–Elmer LS55[®] Spectrofluorimeter using 90° illumination. Initially, prescan was performed¹⁴ to find out the excitation and emission maxima for the silver nanoparticles. Based on the excitation maxima, emission scans were carried out in the range of 500–700 nm. The excitation and emission slit widths were kept at 2.5 and 5.0 nm, respectively, to get the maximum signal-to-noise ratio. The entire scanning was done at the speed of 100 nm/min. The data were analyzed using the FL Winlab[®] software.

3. Results and discussion

It is well known that solutions of polymers can be used for the synthesis and stabilization of nanoparticles. Linear as well as dendritic polymers have been successfully used for nanoparticle synthesis. Polyhydroxylated macromolecules present interesting dynamic supramolecular associations facilitated by inter- and intra-molecular hydrogen bonding resulting in molecular level capsules, which can act as templates for nanoparticle growth.³ Though heparin has been evaluated both as reducing and protecting agent for the preparation of silver

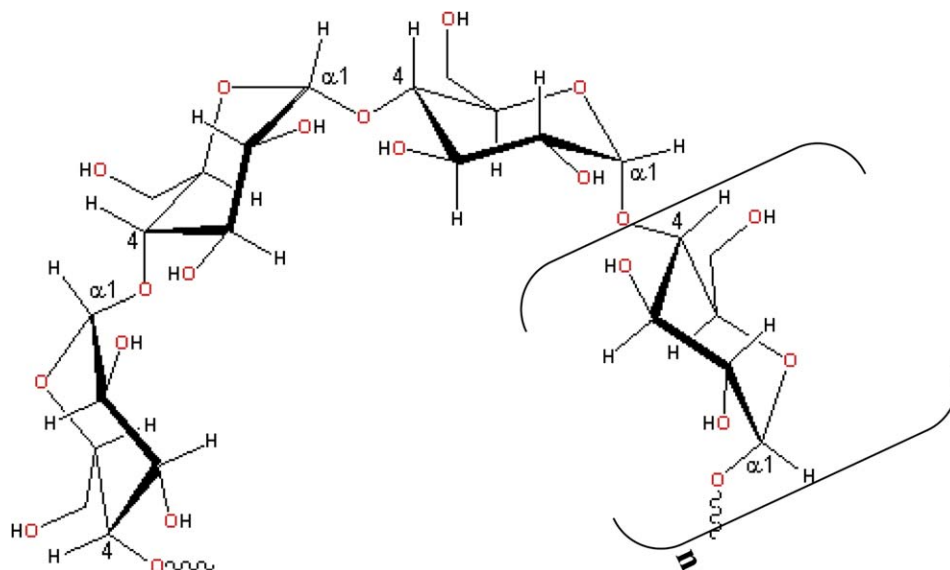


Figure 1. Illustration of the helical structure of amylose chain formed by α -(1 \rightarrow 4) linkages between D-glucose units. Square brackets indicate the monomer.

nanoparticles,¹⁵ no reports have appeared describing the use of soluble starch. The use of soluble starch for the production of silver nanoparticles is very simple and faster. The helical structure of the amylose chain (soluble starch) is depicted in Figure 1. After autoclaving soluble starch with silver nitrate at 15 psi pressure, 121 °C for 5 min, the solution turned yellow, indicating the formation of silver nanoparticles. After complete cooling, the resulting yellow-coloured solution was used for further analysis.

The UV–vis absorption spectrum of this solution is given in Figure 2. The typical peak at 420 nm corresponds to the characteristic surface plasmon resonance of silver nanoparticles. Also, the plasmon band is sym-

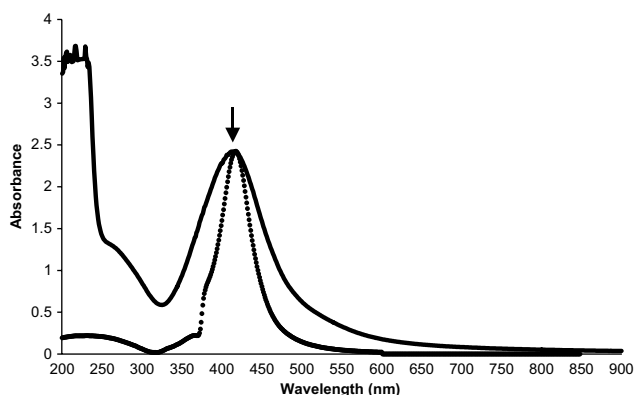


Figure 2. UV–vis absorption spectrum of the silver nanoparticles stabilized using soluble starch. The arrow indicates the maximum absorbance at 420 nm due to the surface plasmon resonance of silver nanoparticles. The dotted line represents the best fit by using the Mie equation.¹⁶

metric, which indicates that the solution does not contain many aggregated particles, a conclusion that agrees with the electron micrograph observation (below). It is well known that colloidal silver nanoparticles exhibit absorption at the wavelength from 390 to 420 nm due to Mie scattering.¹⁶ Hence, the band at 420 nm can be attributed to the property of Mie scattering. We obtained the best-fit spectrum (dotted line in Fig. 2) for the diameter of 23 nm by use of the Mie equation. This value of the diameter is consistent with the estimated average value (22.85 ± 12.94 nm) from the TEM micrographs. This value may not include the protecting agent, i.e., the soluble starch, because the Mie scattering responds only to the silver metal.¹⁷ The plasmon bands are broad with an absorption tail in the longer wavelengths, which could be in principle due to the size distribution of the particles.¹⁸ Since the varying intensity of the plasmon resonance depends on the cluster size, the number of particles cannot be related linearly to the absorbance intensities.¹⁹

We found that increased time and pressure of autoclaving did not influence the formation of silver nanoparticles. Though heating at 100 °C for 5 min was sufficient to synthesize silver nanoparticles, agglomeration occurred within 24 h owing to nonoccurrence of stabilization. It necessitates high temperature/high pressure treatment to expand the starch molecule^{20,21} making it more accessible for silver nanoparticles to get embedded and stabilized. Also, elevated temperature accelerates the reduction process by aldehydes.²² The extensive number of hydroxyl groups present in soluble starch facilitates the complexation of silver ions to the molecular matrix³ while the aldehyde terminals helped in reduction of the same.

The concentration of silver nitrate and soluble starch do not produce any peak shift in the UV–vis spectrum, but the intensity of this peak increased in a nonlinear manner with the concentration of silver nitrate. Above 10 mmol concentration of silver nitrate (for 1.0% starch concentration), agglomeration was noticed indicating the saturation of soluble starch with silver nanoparticles. The stability of the silver nanoparticles stabilized with soluble starch was analyzed by storing the samples at room temperature ($\sim 25^\circ\text{C}$) for 90 days. The absorbance at 420 nm was monitored at an interval of 24 h to check for agglomeration. No significant change (at 1.0% level) in absorbance was noticed during storage indicating the stability of silver nanoparticles.

A typical TEM micrograph of the silver nanoparticles is given in Figure 3a. The selected area electron diffraction pattern (Fig. 3b) showed a diffuse band correspond-

ing to the 'B' polymorph of soluble starch. The diffraction pattern of silver nanoparticles could not be observed, owing to their deep presence inside the soluble starch matrix. With the help of TEM micrographs, the average particle size (Fig. 3c) of silver nanoparticles is estimated to be 22.85 ± 12.94 nm. While the particles less than 10 nm are spherical in shape, the particles above 30 nm have structures of pentagonal biprisms or decahedra, referred to as multiply twinned particles.²³ In general, the particles are isotropic in shape, that is, with a low aspect ratio.

UV–vis spectra taken at different intervals of iodimetric titration confirmed the presence of the silver nanoparticles inside the helical structure of the amylose chain (Fig. 4). The silver nanoparticles embedded in the amylose chain gave a peak at 420 nm (Fig. 4a), while pure iodine and silver iodide produced peaks at 290, 355 nm (Fig. 4b) and 425 nm (Fig. 4c), respectively. When iodine was added to a silver nanoparticles solution stabilized with soluble starch, silver iodide was initially formed (Fig. 4d), making the solution turbid²⁴ and producing an absorption peak at 425 nm. Excess addition of iodine gave a peak at 585 nm in addition to the peaks at 355 and 425 nm (Fig. 4e). This deep-blue colour ($I_{\text{max}} = 585$ nm)²⁵ was due to the complex formation between amylose and iodine; the iodine inside amylose is mostly polyiodide ions, I_3^- or I_5^- . Further addition of excess silver nanoparticles attracted the iodine from the complex resulting in the formation of a peak at 425 nm (corresponds to AgI) and elimination of the peak at 585 nm (Fig. 4f). This proved that the affinity of iodine is very strong towards silver—more than to amylose. Earlier research reported the replacement of the polyaniline nanoparticles from starch using iodine in both the presence and absence of ultrasonic waves.²⁶ In the present study, ultrasonic waves made no difference in the iodimetric titration. The average conformation of amylose in aqueous solution may be viewed as a disordered coil involving many discernible sequences of short-range helical structures that are irregular and labile.¹³ Based on these observations, it can be proposed that the silver nanoparticles were being encapsulated in the same way, as iodine is known to be encapsulated in starch.

In the XRD spectrum (Fig. 5), the broad reflexion at 20° is due to the low crystallinity of the soluble starch, and other peaks are assigned to diffractions from the (111), (200) and (220) planes of face-centred cubic (fcc) silver. The broadening of these peaks is mostly due to the effect of nano-sized particles.²⁷ Since the silver nanoparticles are embedded within soluble starch (as visualized in TEM micrograph), the diffraction intensity of the silver is very low. The lattice constant calculated from this pattern was 4.0893 \AA , a value in agreement with the literature report ($a = 4.086 \text{ \AA}$, Joint Committee on Powder Diffraction Standards file no. 04-0783). Since

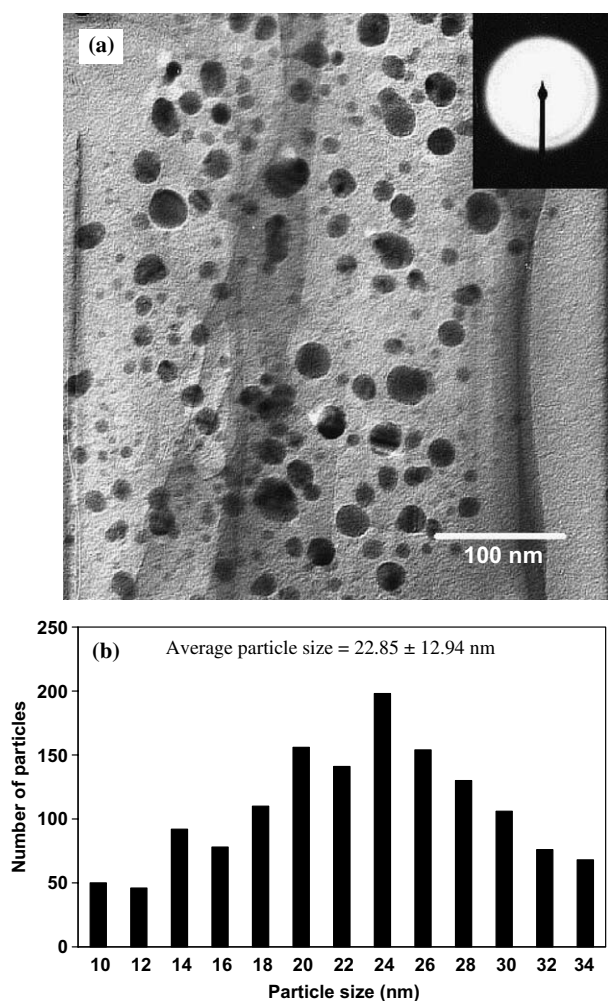


Figure 3. (a) TEM micrograph of the silver nanoparticles embedded in the soluble starch matrix and its corresponding electron diffraction pattern (inset). The diffuse band in the electron diffraction pattern is due to the presence of soluble starch. The scale bar corresponds to 100 nm. (b) Histogram of particle size distribution shows the polydisperse nature of silver nanoparticles.

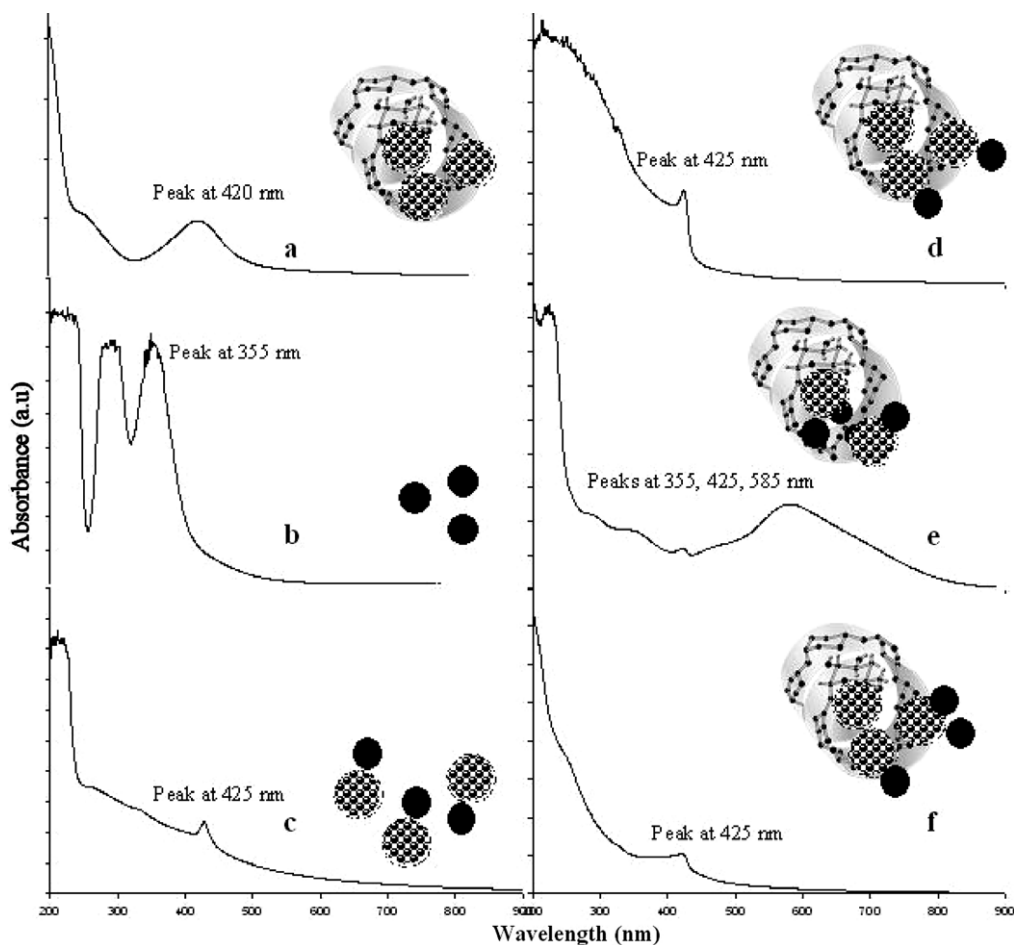


Figure 4. UV-vis spectra of (a) silver nanoparticles, (b) iodine and (c) silver iodide. The starch nanoparticles solution was titrated with iodine, and the UV-vis spectra at various stages are the following: (d) initial stage indicating the formation of AgI, (e) formation of the amylose-iodine complex and (f) the addition of excess silver nanoparticles resulting in AgI. Insets show the schematic representation of models for corresponding processes. The helical chain represents amylose, while the black and dotted circles correspond to iodine and silver nanoparticles, respectively.

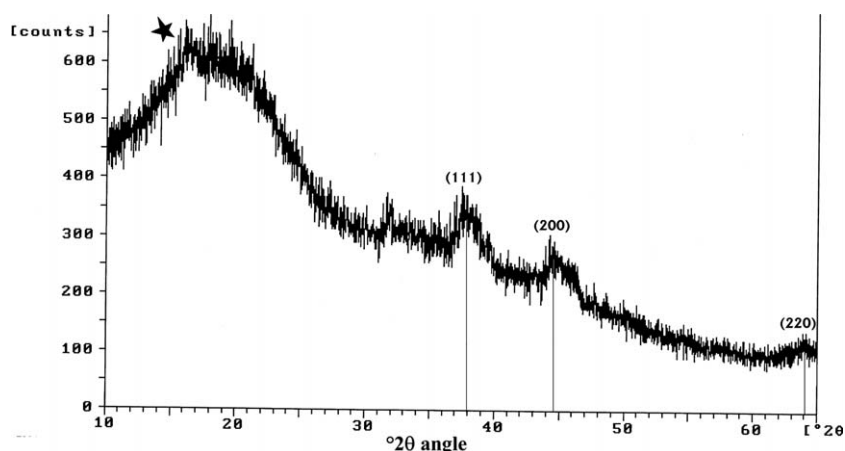


Figure 5. X-ray diffraction pattern of soluble starch impregnated with silver nanoparticles. The peaks assigned to diffractions from the (111), (200) and (220) planes are of fcc silver while the broad peak (★) corresponds to the 'B' polymorph of soluble starch. The X-ray source is Cu K α .

high-amylose starches show low crystallinity (15–22%),²⁸ its diffraction pattern showed a very broad based peak. The crystalline phase of high amylose starch

consists of 74.6–84.6% B-type and 15.4–22.6% V-type polymorphs, while the A type will be produced by high-amylopectin starches.

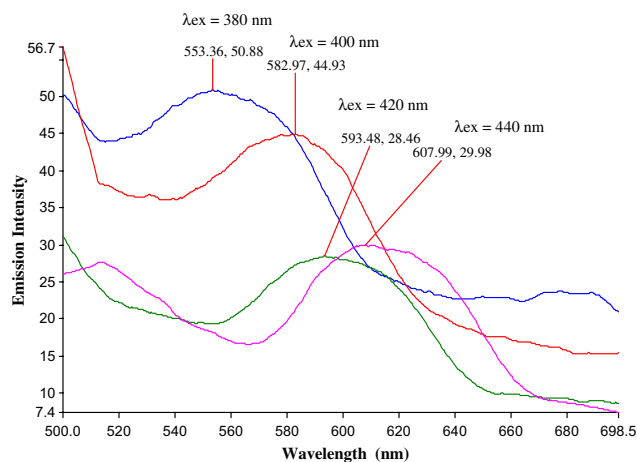


Figure 6. Photoluminescence spectra of silver nanoparticles embedded in soluble starch, while λ_{ex} represents corresponding excitation wavelength, while the legends indicate the emission wavelength (nm) and intensity (a.u.).

The photoluminescence spectra of the silver nanoparticles embedded in soluble starch produced a typical emission peak at 553 nm when excited at 380 nm (Fig. 6). The increased wavelength of excitation resulted in the red shift of the emission peak with a reduction in intensity. This characteristic emission peak was not exhibited by soluble starch alone. Earlier, a characteristic fluorescence peak for the silver nanoparticles in the water phase at 465 nm was reported.²⁹ The red shift in the present work could be attributed to the presence of soluble starch as a capping agent.

The three main steps in the preparation of nanoparticles that should be evaluated from a green chemistry perspective are the choice of the solvent medium used for synthesis, the choice of an environmentally benign reducing agent, and the choice of a nontoxic material for the stabilization of nanoparticles. The use of soluble starch for synthesis and stabilization of silver nanoparticles completely avoided the use of organic solvents and other harmful reducing agents. Also, the binding interaction between soluble starch and silver nanoparticles is relatively weak compared to the interaction between the nanoparticles and typical thiol-based protecting groups.³ This implies that the protection should be easily reversible, enabling the separation of these nanoparticles.

4. Conclusions

Green chemistry aims at the total elimination or at least the minimization of generated waste and the implementation of sustainable processes through the adoption of 12 fundamental principles.³⁰ In this work, we have reported a novel, one-pot synthetic route to prepare silver nanoparticles, reduced and stabilized by soluble starch.

Nanoparticles thus prepared are found to be stable in solution over a period of three months at room temperature ($\sim 25^\circ\text{C}$) and show no signs of aggregation. The use of environmentally benign and renewable materials like soluble starch offers numerous benefits of eco-friendliness and compatibility for pharmaceutical and biomedical applications. Moreover, the widespread occurrence of these naturally occurring polysaccharide makes this process amenable to large-scale industrial production.

Acknowledgements

We gratefully acknowledge the guidance provided by Dr. S. Sreenivasan, Director CIRCOT and technical support rendered by Mr. Virendra Prasad, Mr. C. Sundaramoorthy, Mr. Sekar, Mr. Vivekanandan and Mr. R. P. Kadam in carrying out the experiments and analysis. We acknowledge the staffs of Sophisticated and Instrumentation Facility at Indian Institute of Technology, Mumbai, for their help in analysis of nanoparticles by TEM.

References

1. Poliakoff, M.; Anastas, P. *Nature* **2001**, *413*, 257.
2. DeSimone, J. M. *Science* **2002**, *297*, 799–803.
3. Raveendran, P.; Fu, J.; Wallen, S. L. *J. Am. Chem. Soc.* **2003**, *125*, 13940.
4. Lewis, L. N. *Chem. Rev.* **1993**, *93*, 2693–2730.
5. Henglein, A. *Chem. Rev.* **1989**, *89*, 1861–1873.
6. Alivisatos, A. P. *Science* **1996**, *271*, 933–937.
7. Huang, H.; Yuan, Q.; Yang, X. *Colloids Surf. B: Biointerfaces* **2004**, *39*, 31–37.
8. Mandal, S.; Phadtare, S.; Sastry, M. *Curr. Appl. Phys.* **2005**, *5*, 118–127.
9. Taton, T. A.; Mirkin, C. A.; Letsinger, R. L. *Science* **2000**, *289*, 1757–1760.
10. Cao, Y. C.; Jin, R.; Mirkin, C. A. *Science* **2002**, *297*, 1536–1540.
11. Chan, W. C. W.; Nie, S. *Science* **1998**, *281*, 2016–2018.
12. Sandhu, K. K.; McIntosh, C. M.; Simard, J. M.; Smith, S. W.; Rotello, V. M. *Bioconjugate Chem.* **2002**, *13*, 3–6.
13. Walter, R. H. *Polysaccharide Association Structures in Food*; Marcel Dekker: New York, 1998.
14. Vigneshwaran, N.; Bijukumar, G.; Karmakar, N.; Anand, S.; Misra, A. *Spectrochim. Acta, Part A* **2005**, *61*, 163–170.
15. Huang, H.; Yang, X. *Carbohydr. Res.* **2004**, *339*, 2627–2631.
16. Kleemann, W. *Int. J. Mod. Phys. B* **1993**, *7*, 2469.
17. Aoki, K.; Chen, J.; Yang, N.; Nagasawa, H. *Langmuir* **2003**, *19*, 9904–9906.
18. Chalmers, J. M.; Griffiths, P. R. *Handbook of Vibrational Spectroscopy*; Wiley: New York, 2002.
19. Klabunde, K. J. *Nanoscale Materials in Chemistry*; Wiley: New York, 2001.
20. Doi, S.; Clark, J. H.; Macquarrie, D. J.; Milkowski, K. *Chem. Commun. (Cambridge)* **2002**, 2632–2633.
21. Han, J. A.; BeMiller, J. N.; Hamaker, B.; Lim, S. T. *Cereal Chem.* **2003**, *80*, 323–328.

22. Nath, S.; Ghosh, S. K.; Panigrahi, S.; Pal, T. *Indian J. Chem. Sec. A: Inorg., Bio-inorg., Phys., Theor. Anal. Chem.* **2004**, *43*, 1147–1151.
23. Temgire, M. K.; Joshi, S. S. *Radiat. Phys. Chem.* **2001**, *71*, 1039–1044.
24. Skoog, D. A.; West, D. M.; Holler, F. J. *Fundamentals of Analytical Chemistry*, 7th ed.; Harcourt Asia Pvt. Ltd: Singapore, 1996.
25. Banks, W.; Greenwood, C. T. *Starch and its Components*; Edinburg University Press: Edinburg, 1975.
26. Sarma, T. K.; Chattopadhyay, A. *Langmuir* **2004**, *20*, 4733.
27. Prasad, V.; D'Souza, C.; Yadav, D.; Shaikh, A. J.; Vigneshwaran, N. *Spectrochim. Acta, Part A* **2006**, *65*, 173–178.
28. Zobel, H. F. *Starch/Stärke* **1988**, *40*, 44–50.
29. Jiang, Z.; Yuan, W.; Pan, H. *Spectrochim. Acta, Part A* **2005**, *61*, 2488–2494.
30. Anatas, P. T.; Warner, J. C. *Green Chemistry: Theory and Practice*; Oxford University Press: New York, 1998.